

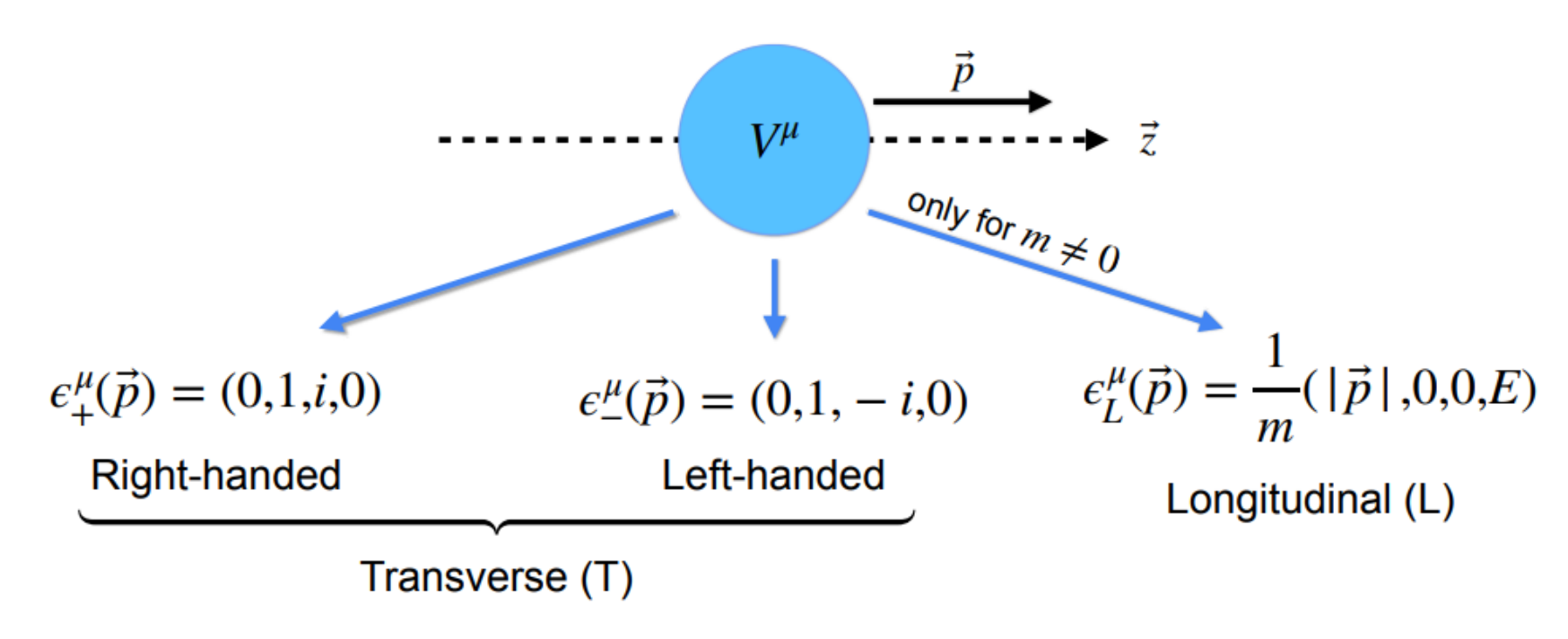


Polarisation measurements of the same-sign WW vector boson scattering at $\sqrt{s} = 13 \, TeV$ with the ATLAS detector

[PHYSICAL REVIEW LETTERS 135, 111802 (2025)]

Zhanhang Zhou, University of Science and Technology of China 2025/11/1

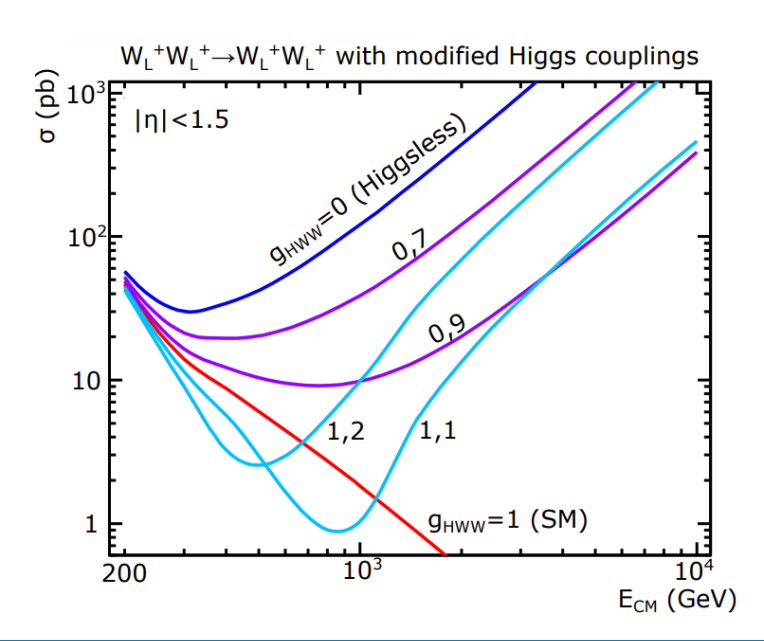
Vector boson polarization state

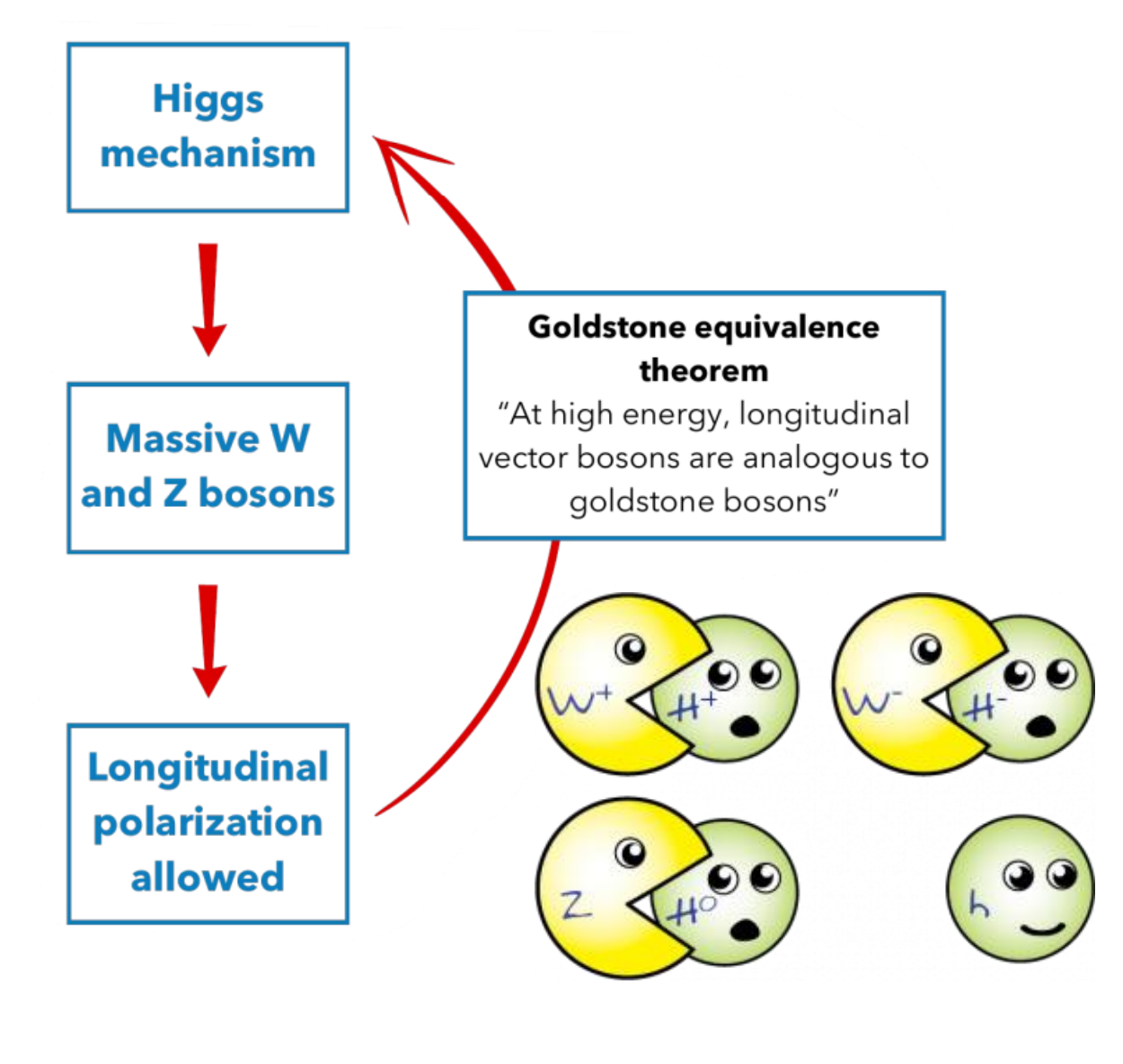


- Polarization: alignment of a particle's spin with its momentum
- For the massive vector boson, helicity: $h = \vec{S} \cdot \frac{\vec{p}}{|\vec{p}|}$
 - Transverse (T): $h = \pm 1$
 - Longitudinal (L): h = 0

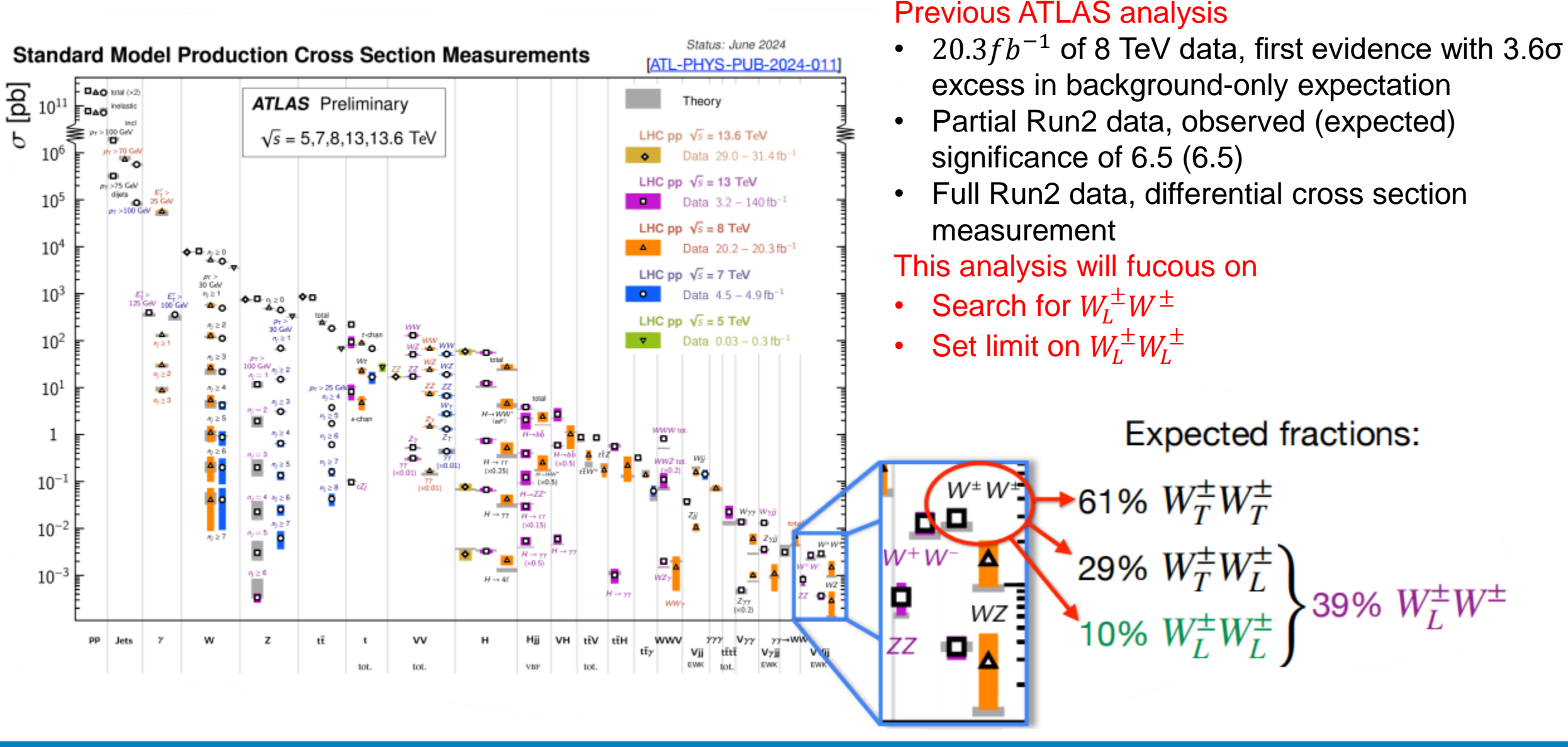
Importance of polarization state

- Existence of Higgs boson is discovered in 2012
- Developing a deeper understanding of the electroweak symmetry breaking (EWSB) mechanism is crucial
- The longitunial polarization state of W^{\pm} and Z bosons is a direct consequence of the Higgs machanism
- Import test of Higgs machanism
- Particularly interesting: longitudinal VBS

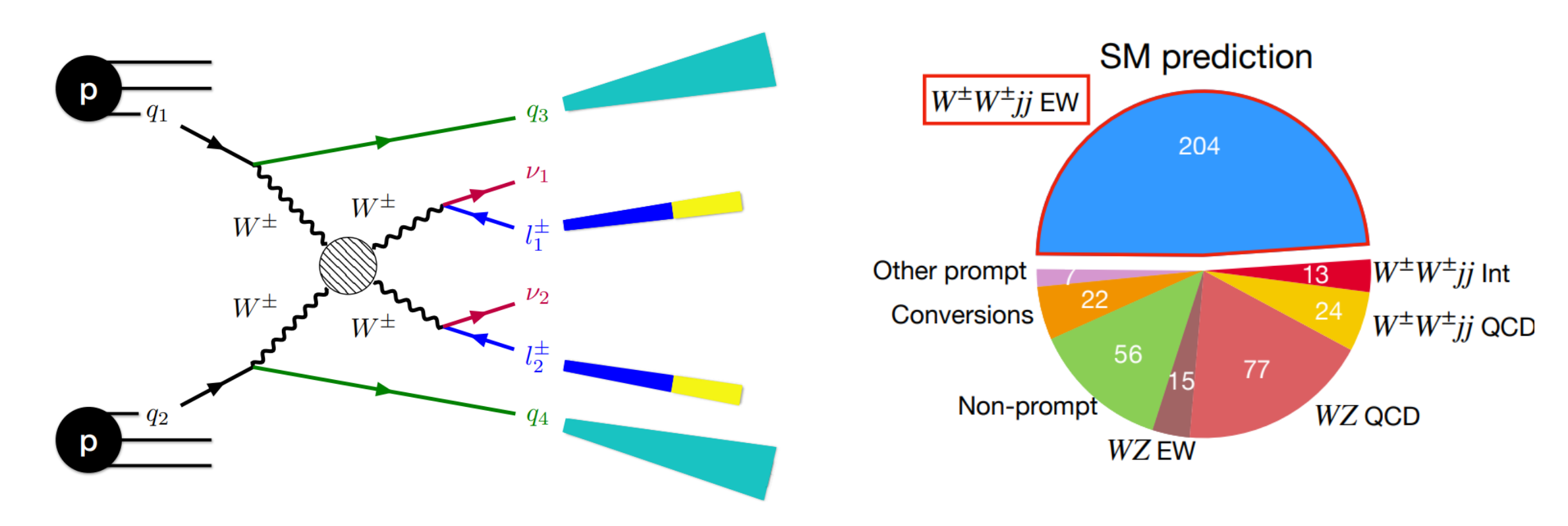




ATLAS study on $pp \rightarrow W^{\pm}W^{\pm}jj$



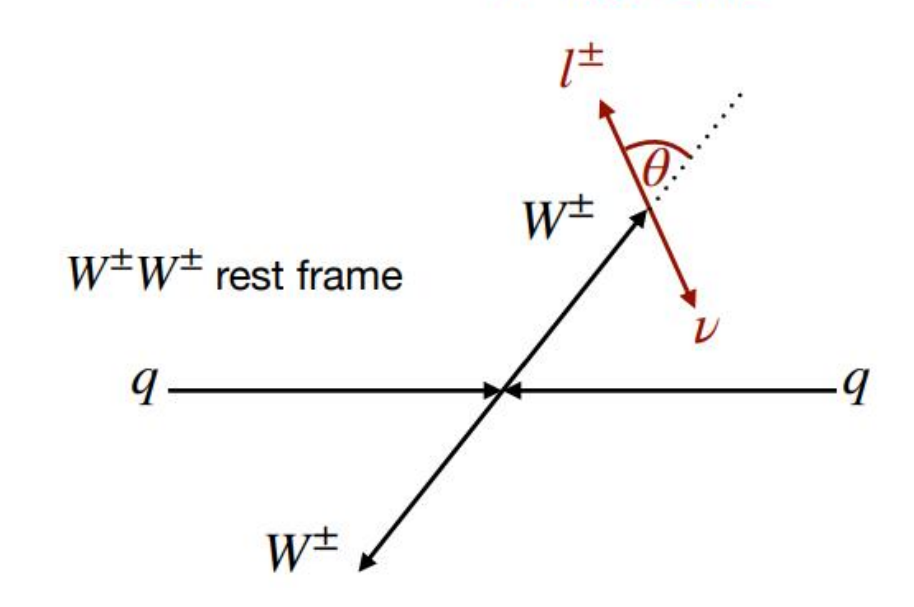
Signature of $pp \rightarrow W^{\pm}W^{\pm}jj$



- Full Run 2 data is used. Basically follow the strategy of $pp \to W^{\pm}W^{\pm}jj$ cross section measurement
- Exactly two same charged leptons with $p_T > 27 \; GeV$
- At least two well-seperated jets with Mjj > 500 GeV, $|\Delta Yjj| > 2$
- Missing transverse momentum $E_T^{miss} > 30 GeV$

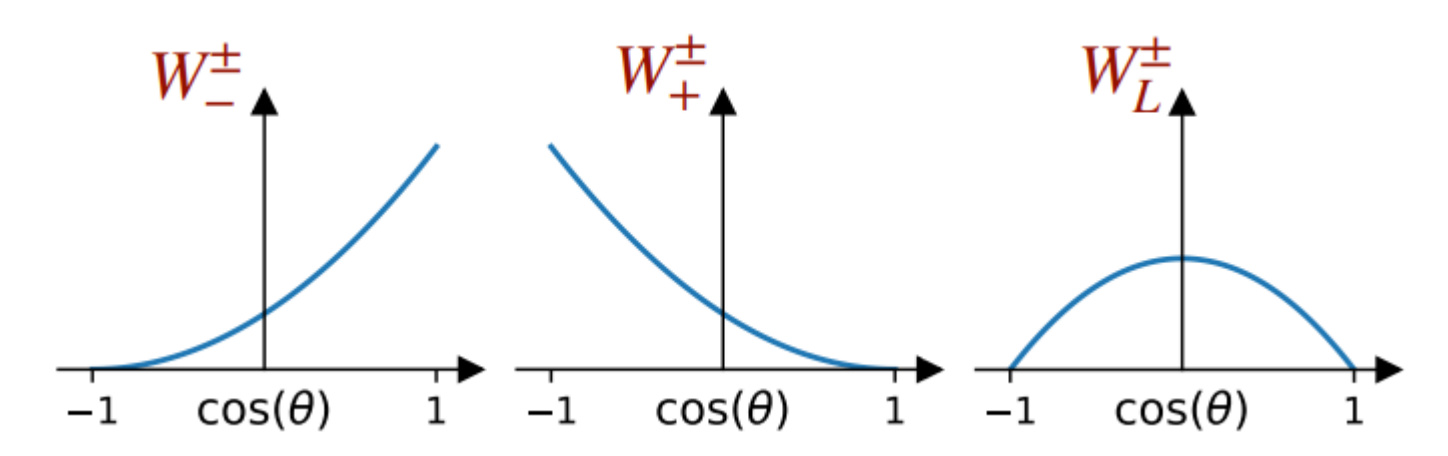
Acess polarization information

- W^{\pm} polariztaion state determine the decay angle distribution
 - But can not access W^{\pm} rest frame since the two neutrinos are not reconstructable
 - Simulate full event kinematic of polarization states prediceted by MC
- Two key points
 - Simulation of polarization state
 - Distinguish the polarization state



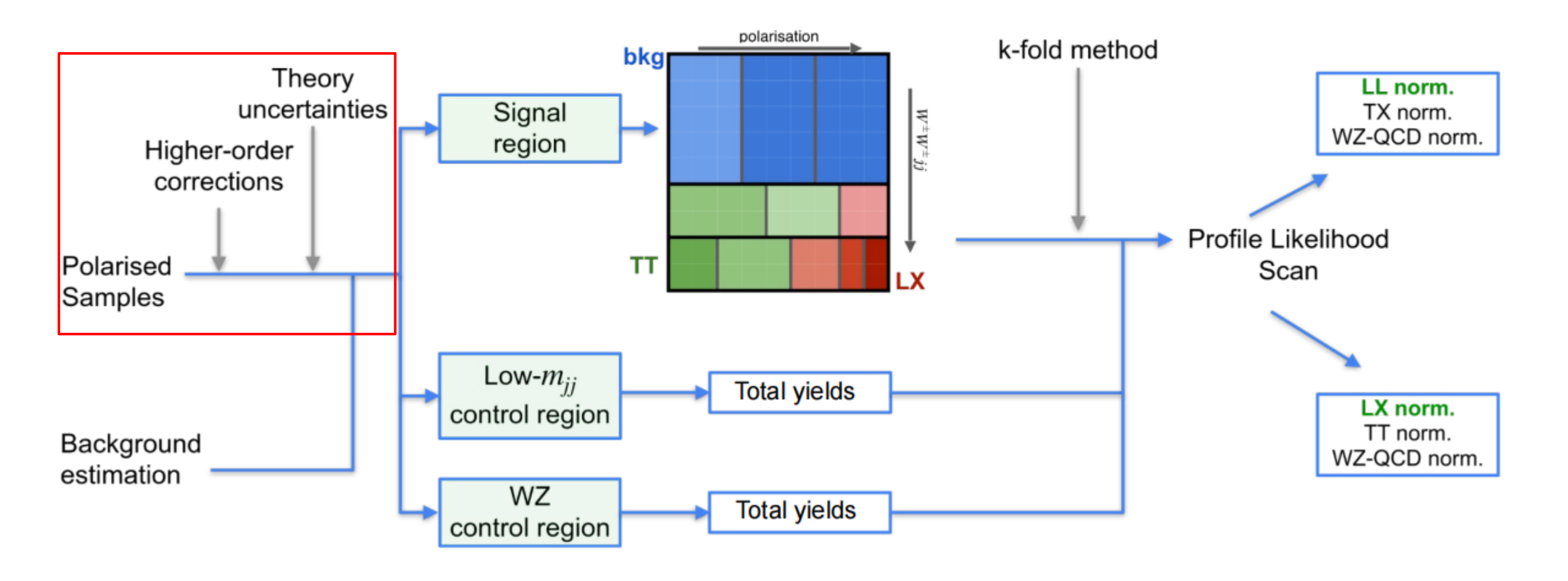
 W^{\pm} rest frame

6



Analysis strategy

2D DNN application

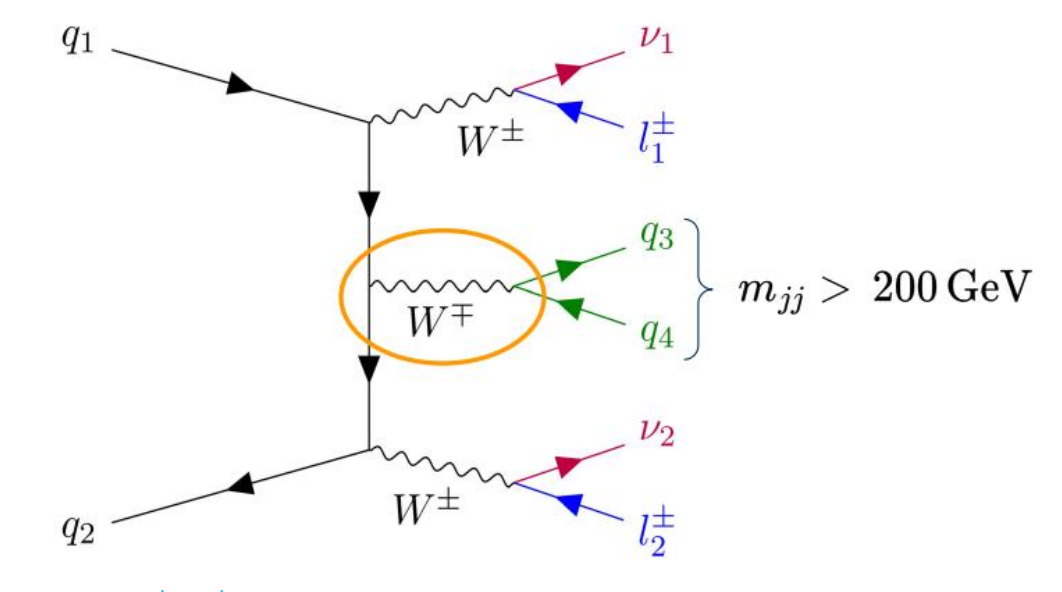


Polarized $W^{\pm}W^{\pm}jj$ sample

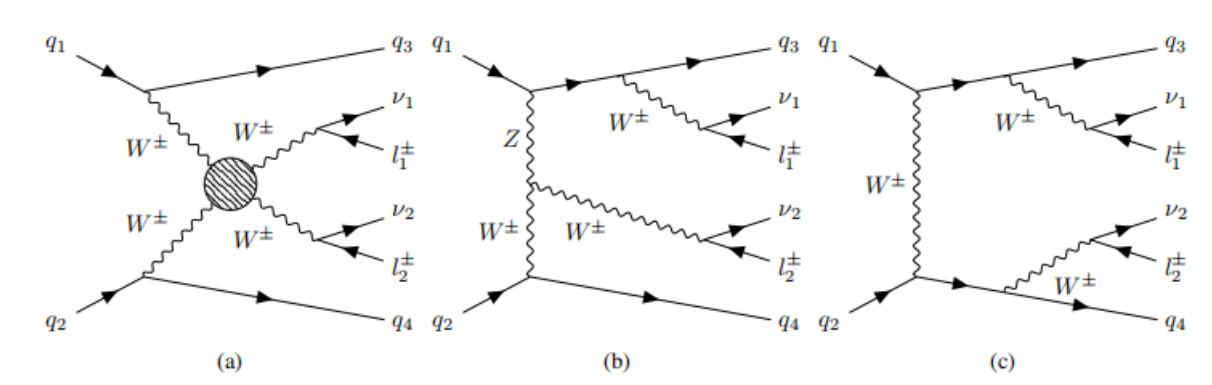
- Sherpa3 can generate LO ($\alpha_W = 6$) polarized $W^{\pm}W^{\pm}jj$ sample
 - On-shell and narrow and narrow-width approximation (NWA) necessary

$$rac{1}{\left(q^2-m_V^2
ight)^2\,+\,\Gamma_V^2m_V^2}\,
ightarrow\,rac{\pi\delta\left(q^2-m_V^2
ight)}{\Gamma_V m_V}$$

- Vector boson width set to zero to ensure gauge invariance
 - \rightarrow divergent at $m_{qq} = m_W$
 - \rightarrow avoid by the $m_{ij} > 200 GeV$ selection in SR



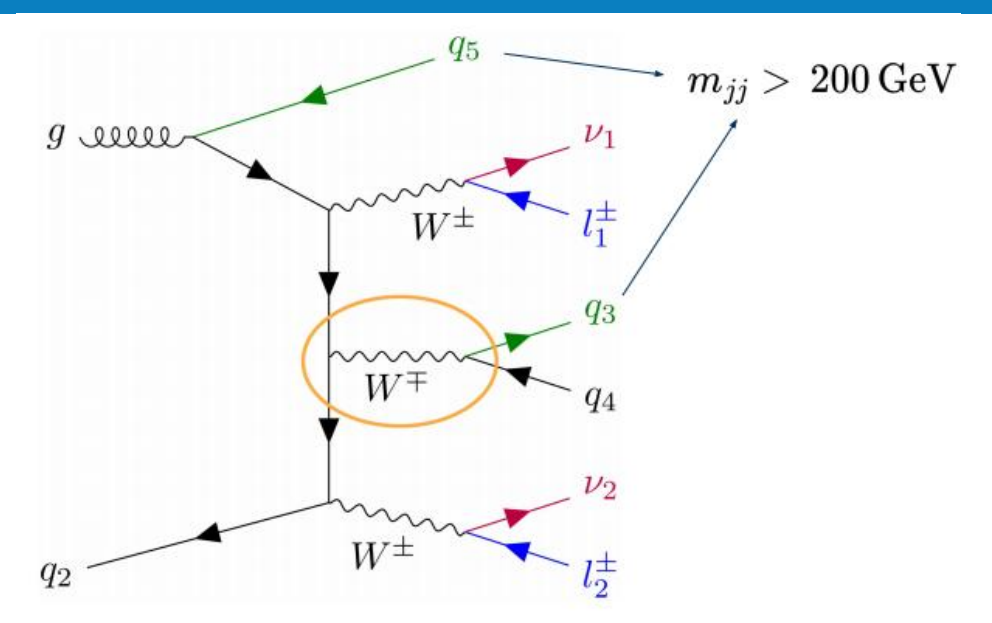
Typical $W^{\pm}W^{\pm}jj-EW$ Feynman diagram with the hadronically decaying W^{\pm} in the s-channel-like diagram

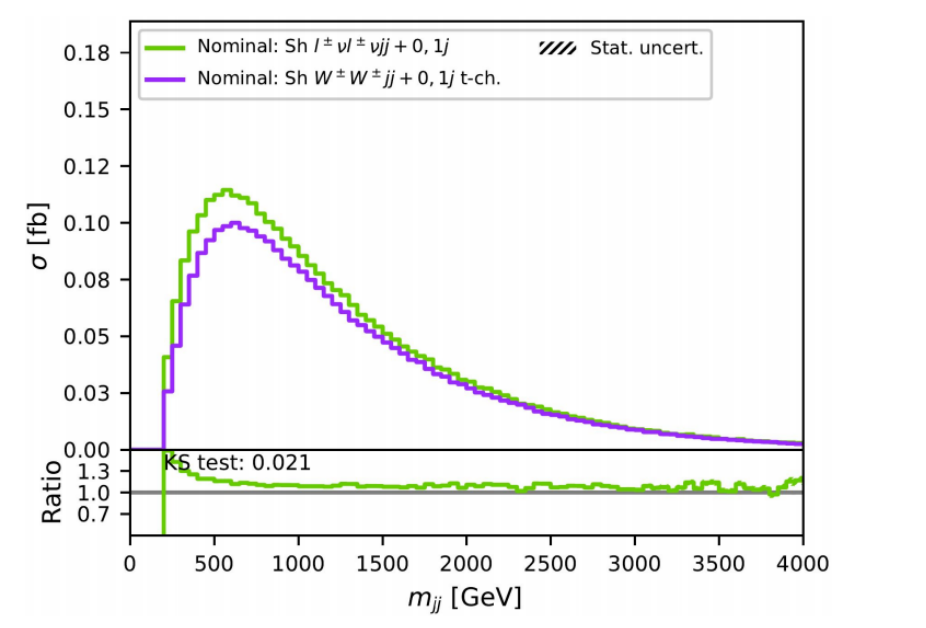


Typical $W^{\pm}W^{\pm}jj-W$ Feynman diagrams without hadronically decaying W^{\pm} in the s-channel

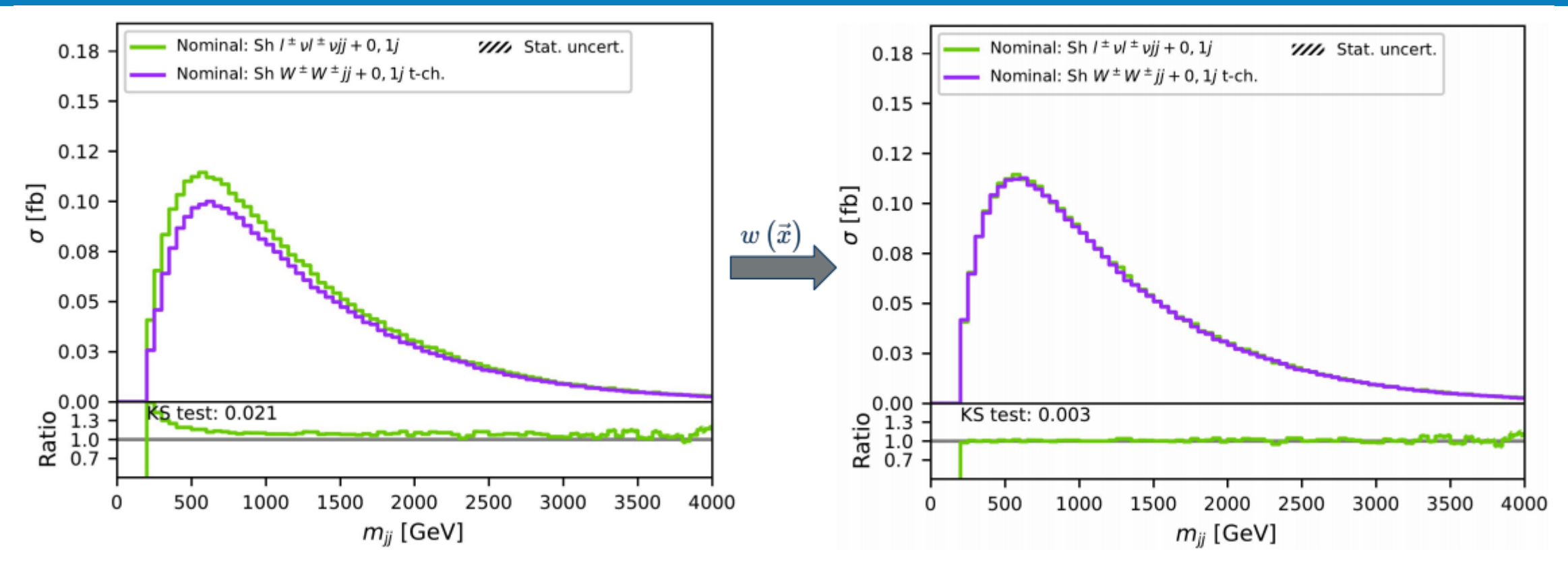
High-order QCD correction

- Simulate $W^{\pm}W^{\pm}jj + 0.1j$
- The multijet merging is expected to cover the dominant higher-order QCD effect
- Problem:
 - At higher order QCD, the NWA approximation can lead to divergences if two leading jets do not originated from the W[±]
- Solution:
 - 1. The s-channel diagrams are dropped for the polarizatio simulation with higher-order QCD
 - 2. Full off-shell $l^{\pm}l^{\pm}vvjj + 0.1j$ to correct missing schannels





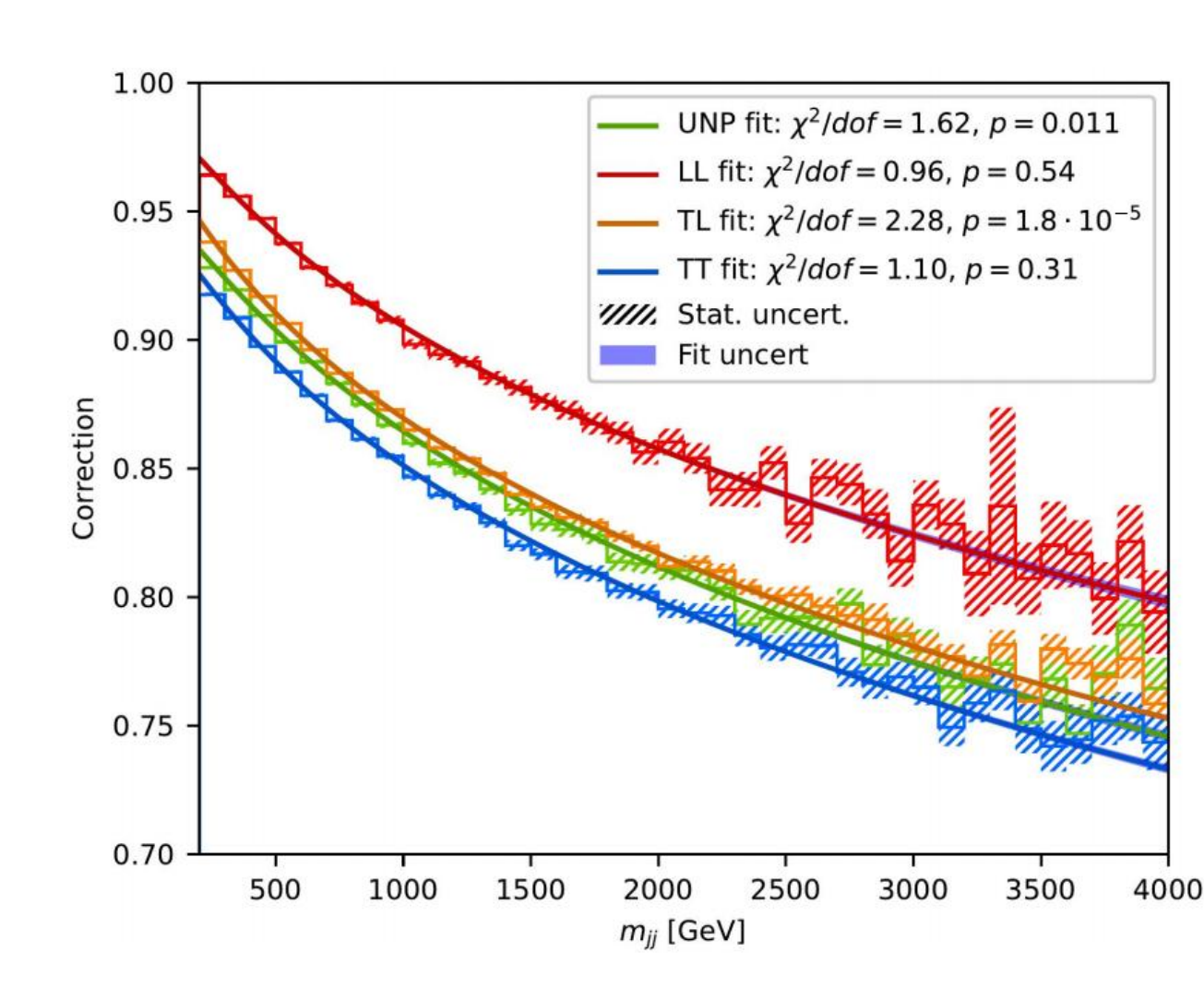
High-order QCD correction



- The MVA classifier is used to discriminate signal → Full phase-space reweighting using DNN is needed
 - Likelihood-ratio can be approximated using binary classifier $\frac{p_1}{p_2} \sim \frac{DNN(x)}{1-NN(x)}$ [https://arxiv.org/abs/1907.08209]
- For our implementation
 - DNN_{s-h} : $l^{\pm}l^{\pm}vvjj + 0,1j$ VS $W^{\pm}W^{\pm}vvjj + 0,1j$
 - $\omega(\vec{x}) = \frac{DNN_{s-h}(x)}{1 DNN_{s-h}(x)}$

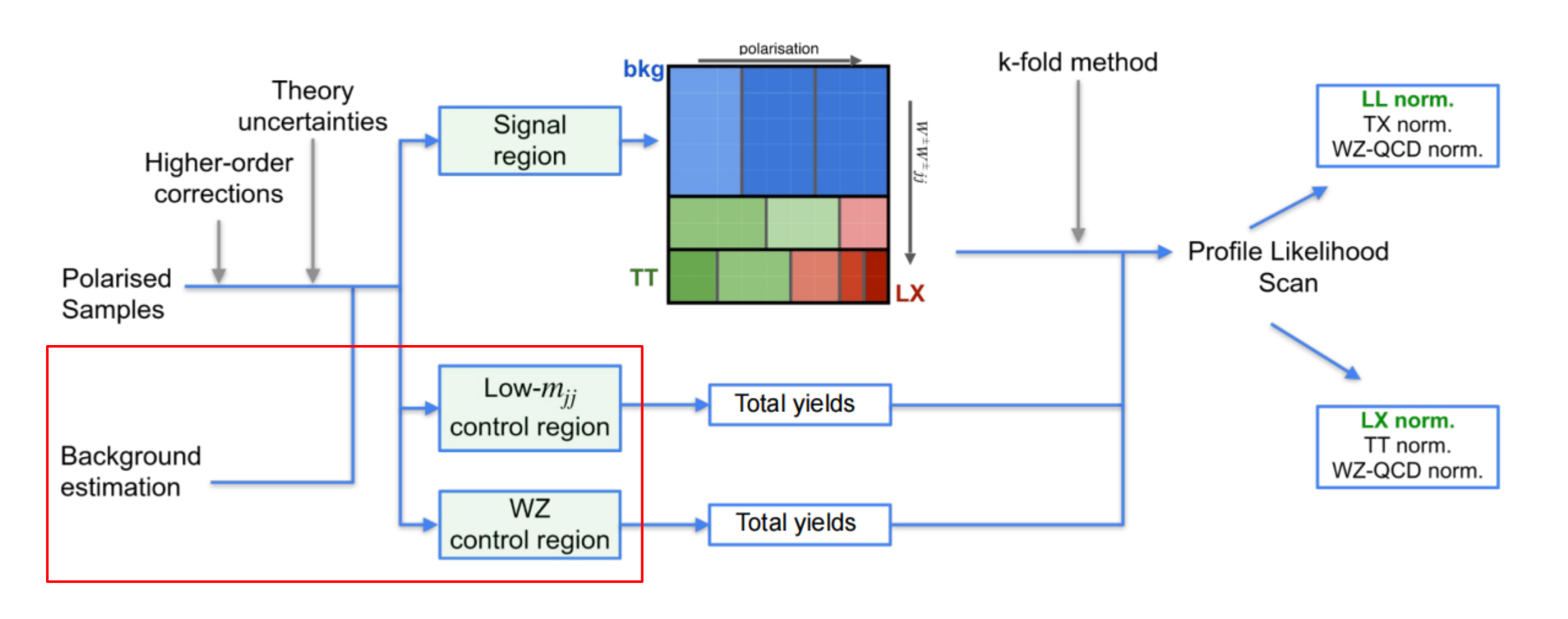
NLO EW correction

- Polarized NLO EW correction provided by [https://arxiv.org/pdf/2409.03620]
- The comparision f of the m_{jj}-dependent differential cross-section of W[±]W[±]jj W at Born level (O(α_W = 6)) and at NLO-EW(up to O(α_W = 7)) is used to weight events
- Perform separate fit for each polarization $f(m_{jj})=p_0+p_1ln\frac{m_{jj}}{GeV}+p_2ln^2\frac{m_{jj}}{GeV}$



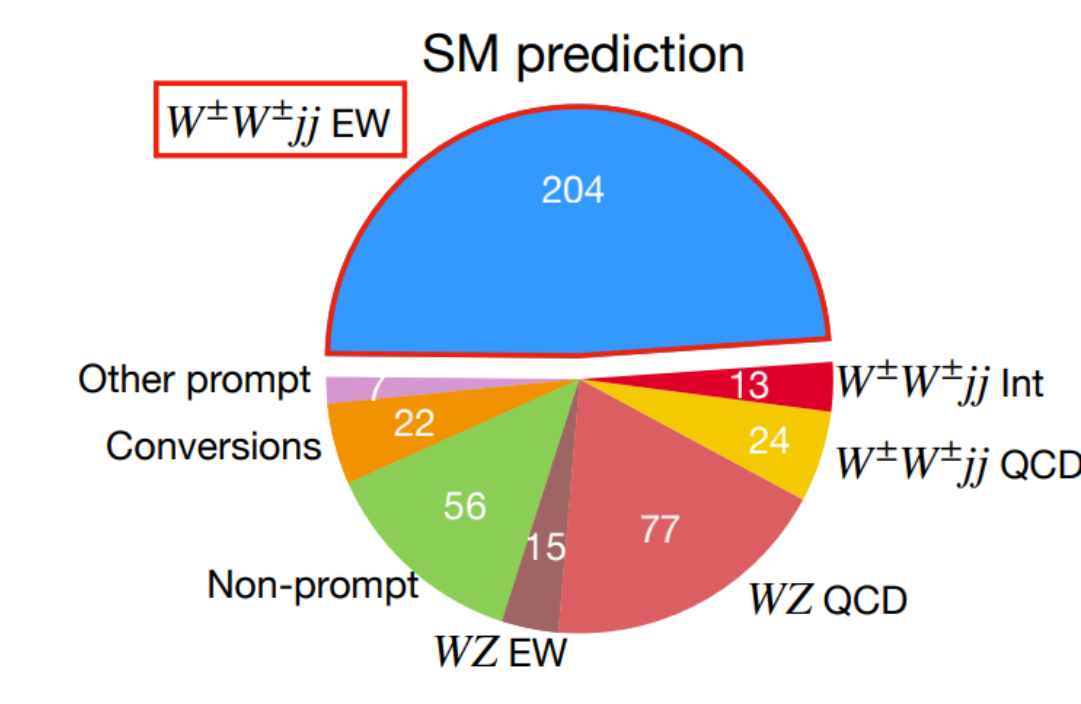
Analysis strategy

2D DNN application



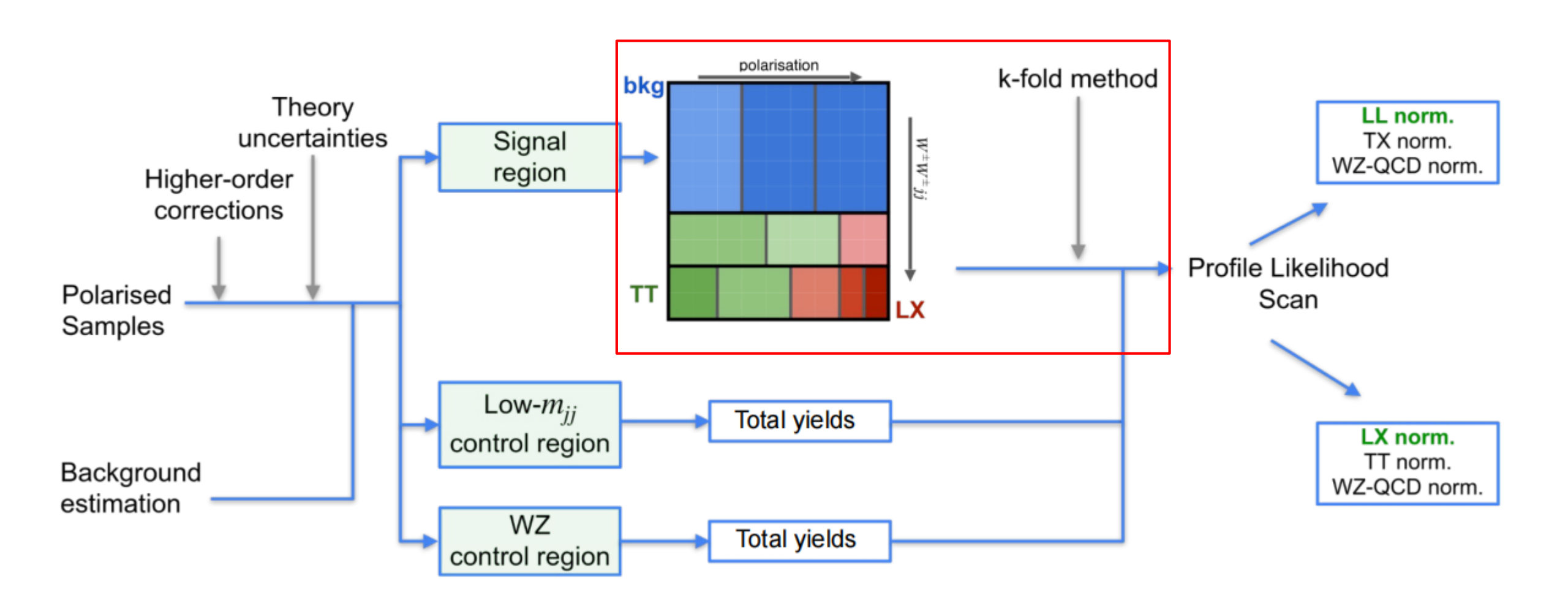
Background estimation

- Monte Carlo simulation:
 - W[±]W[±]jj QCD and Interference
 - W[±]Z QCD and EW
 - Other minor prompt contribution
- Data-driven estimation
 - Non-prompt events: jet/photon misidentified as lepton
 - Conversion events: lepton charge misidentified
- Two Control Regions are defined and taken into account for the fit to constrain background
 - Low Mjj CR: equivalent to SR but with a lower dijet mass 200 GeV < Mjj < 500 GeV
 - WZ CR: equivalent to SR but with an extra opposite-sign charge lepton

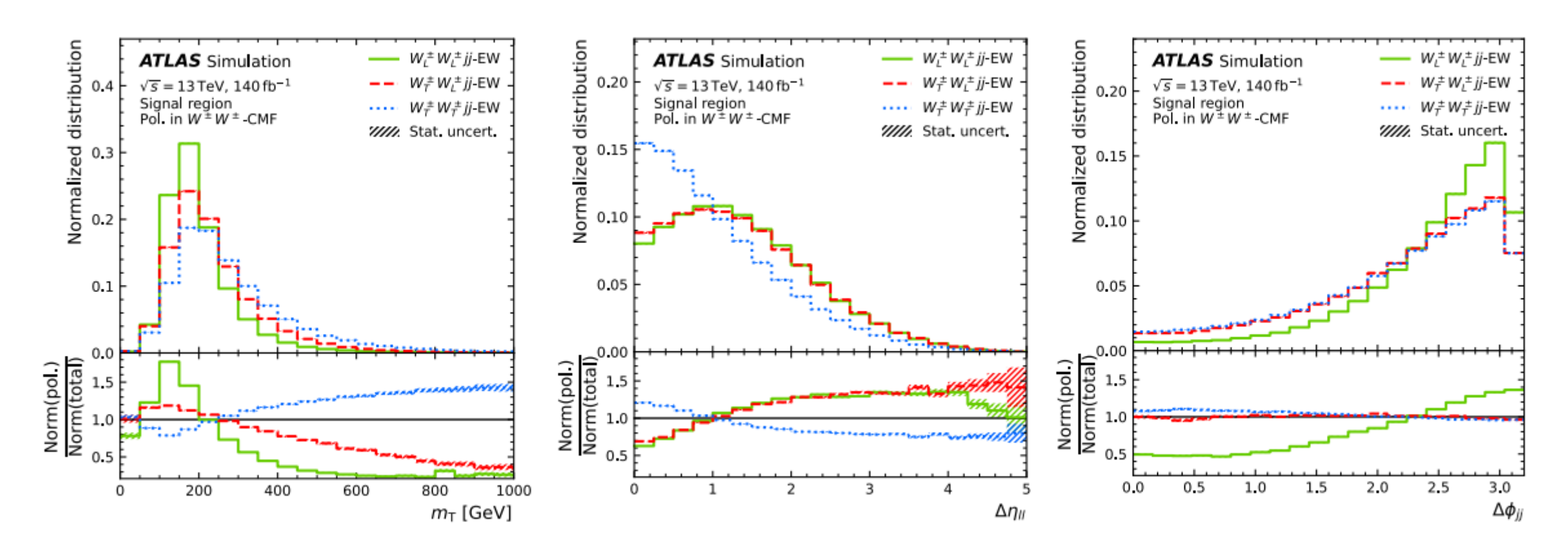


Analysis strategy

2D DNN application



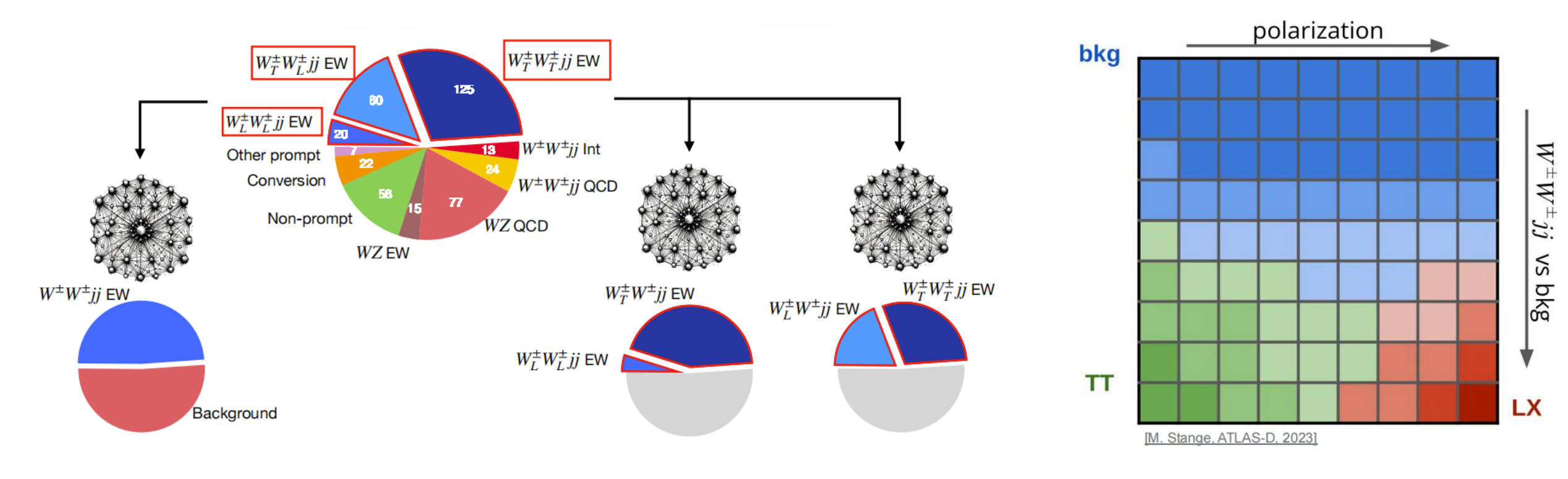
Signal discriminant



- The polarization of W^{\pm} determine its decay angle distribution ==> lepton kinematic and MET can discriminate W^{\pm} polarization state
- The initial W^{\pm} bosons are connected to the quark lines ==> jet kinematic can discriminate W^{\pm} polarization state

Maximize the senstivity through combination in DNN

MVA classifier

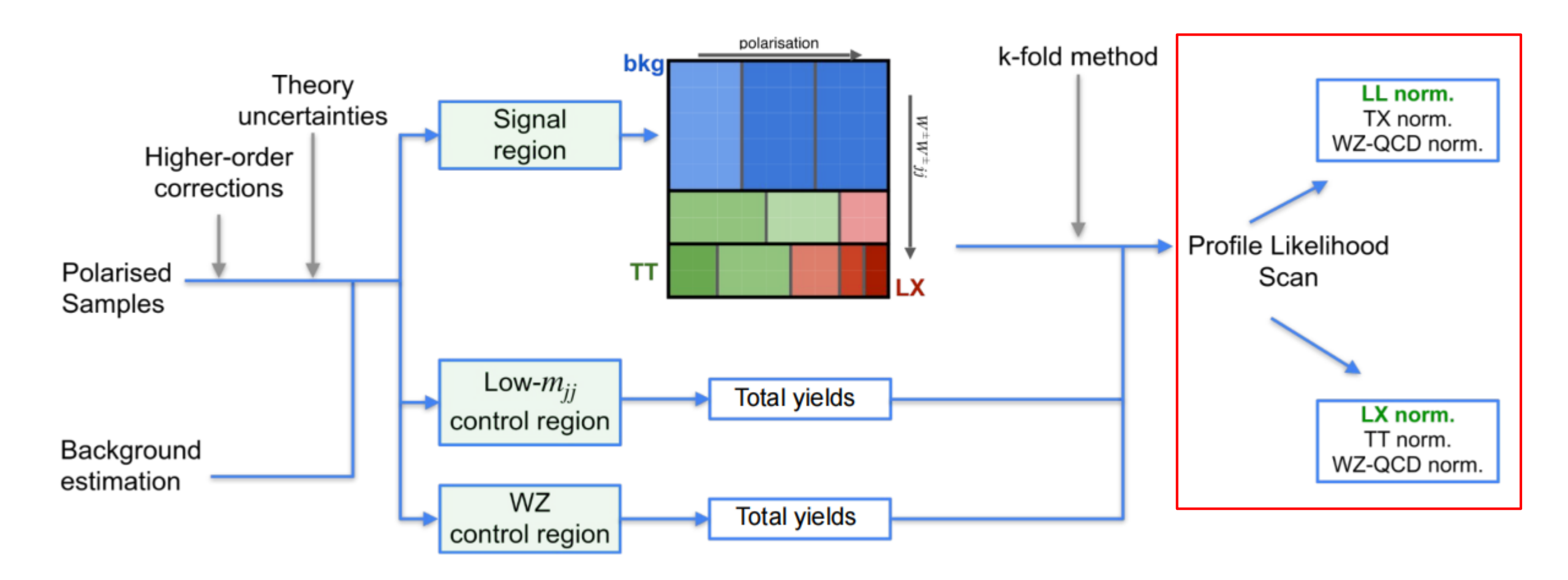


- Three sets of DNNS are trained to extract the polarization components:
 - DNN_{inclusive}, used to separate the unpolarized $W^{\pm}W^{\pm}jj EW$ contribution from the remaining background
 - DNN_{LL}, used to seperate fully longitudinal polarized $W_L^{\pm}W_L^{\pm}jj-EW$ simulation from the contribution with at lest one transversely-polarized state $W_T^{\pm}W^{\pm}jj-EW$
 - DNN_{LL}, used to seperate the polarization state $W_L^{\pm}W^{\pm}jj EW$ simulation from the contribution with fully transversely-polarized state $W_T^{\pm}W^{\pm}jj EW$

2D histogram from classifier score

Analysis strategy

2D DNN application



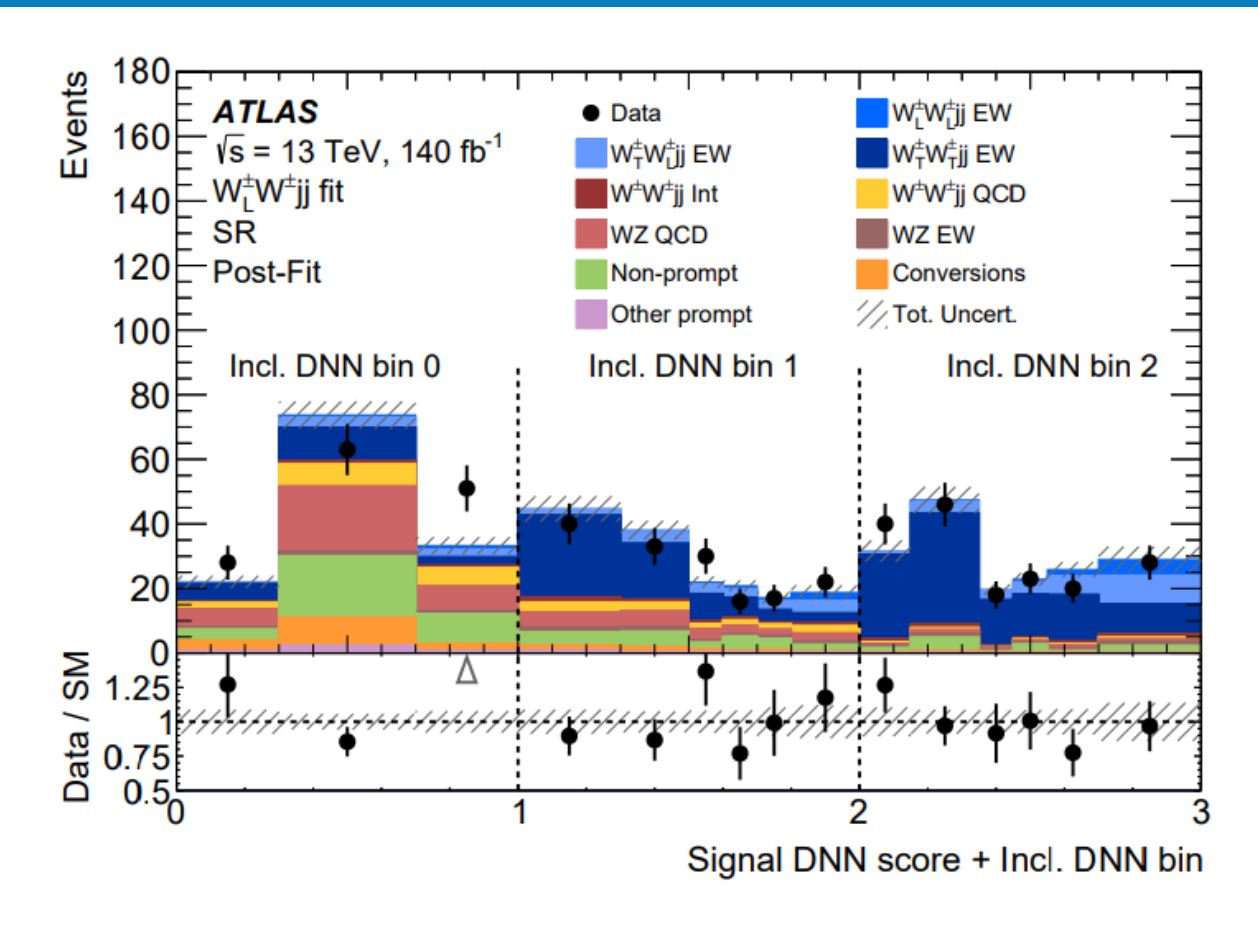
Profile likelihood procedure

$$\mathcal{L}(\mu, \vec{\theta}) = \prod_{i}^{bins} \mathcal{L}_{poiss}(N_{data}|\mu s(\theta) + \mu_{b}b(\theta))_{i} \times \mathcal{L}_{gauss}(\theta)_{i}.$$

- To extract the signal component contribution from background, profile likelihood fits are performed
- The systematical uncertainty ebter the fit via Gasssian constrain as nuisance parameter
- Two POI fitting
 - Search for $W_L^{\pm}W^{\pm}$: 3 normalization factors for $W_L^{\pm}W^{\pm}jj\;EW$, $W_T^{\pm}W_T^{\pm}jj\;EW$, background
 - Set limit on $W_L^{\pm}W_L^{\pm}$: 3 normalization factors for $W_L^{\pm}W_L^{\pm}jj\;EW$, $W_T^{\pm}W^{\pm}jj\;EW$, background

Result of single boson polarizatoin $W_L^{\pm}W^{\pm}$

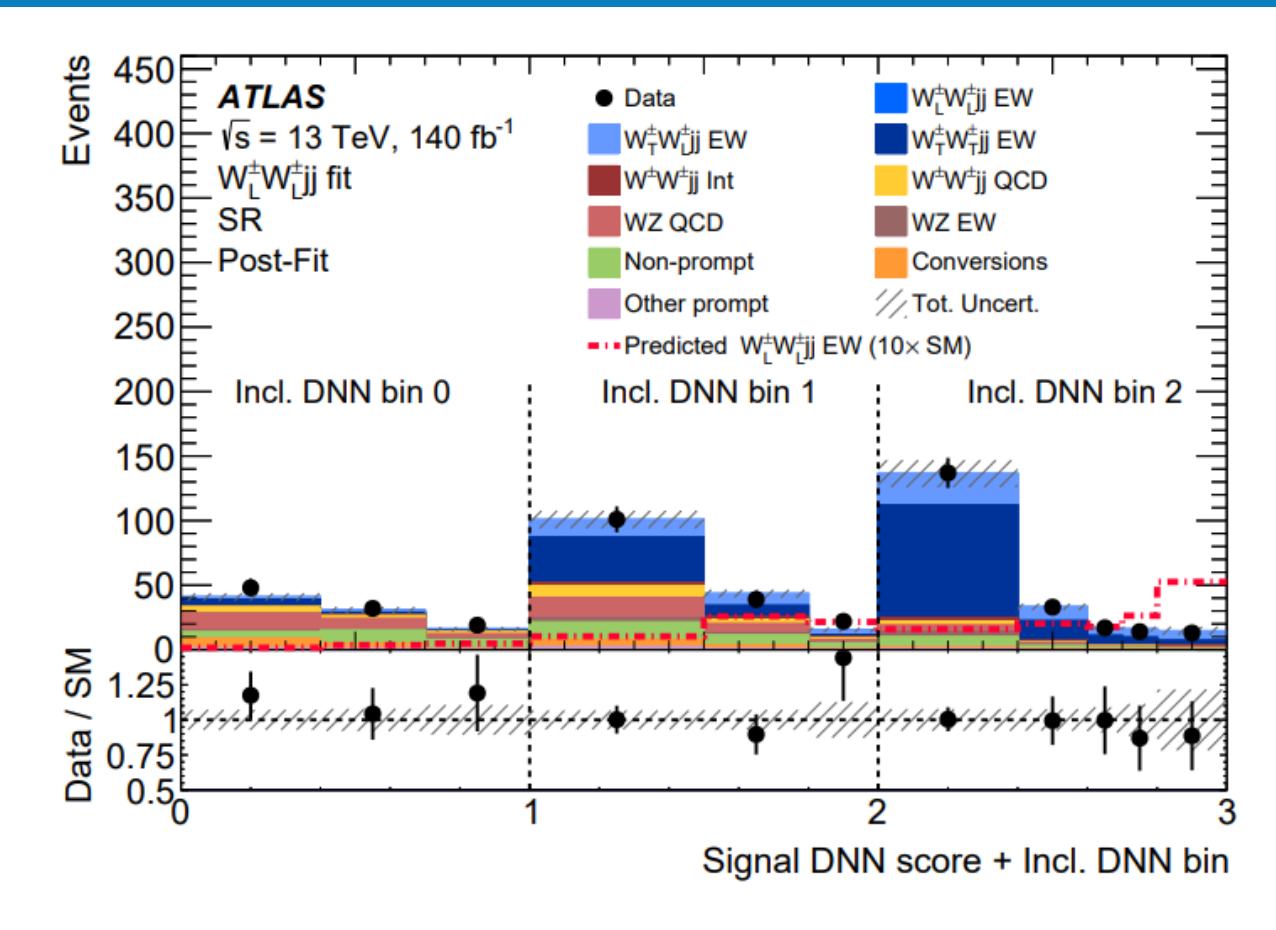
- Significance of 3.3σ for $W_L^{\pm}W^{\pm}jj$ (expected 4.0σ)
 - First evidence for longitudinal polarization in vector boson scattering
- Fiducial cross sections are measured, in agreement with the Stand Model
- Dominated by statistical uncertainty



Process	Predicet σB [fb]	Measured σB [fb]	Uncertainty
$W_L^{\pm}W^{\pm}jj-W$	1.18±0.29	0.88±0.30(tot)	± 0.28 (stat) ± 0.05 (mod.sys) ± 0.08 (exp.sys)
$W_T^{\pm}W_T^{\pm}jj$ - EW	1.67±0.40	2.49±0.32(tot)	$\pm 0.30(\text{stat})\pm 0.05(\text{mod.sys})\pm 0.12(\text{exp.sys})$

Result of single boson polarizatoin $W_L^{\pm}W_L^{\pm}$

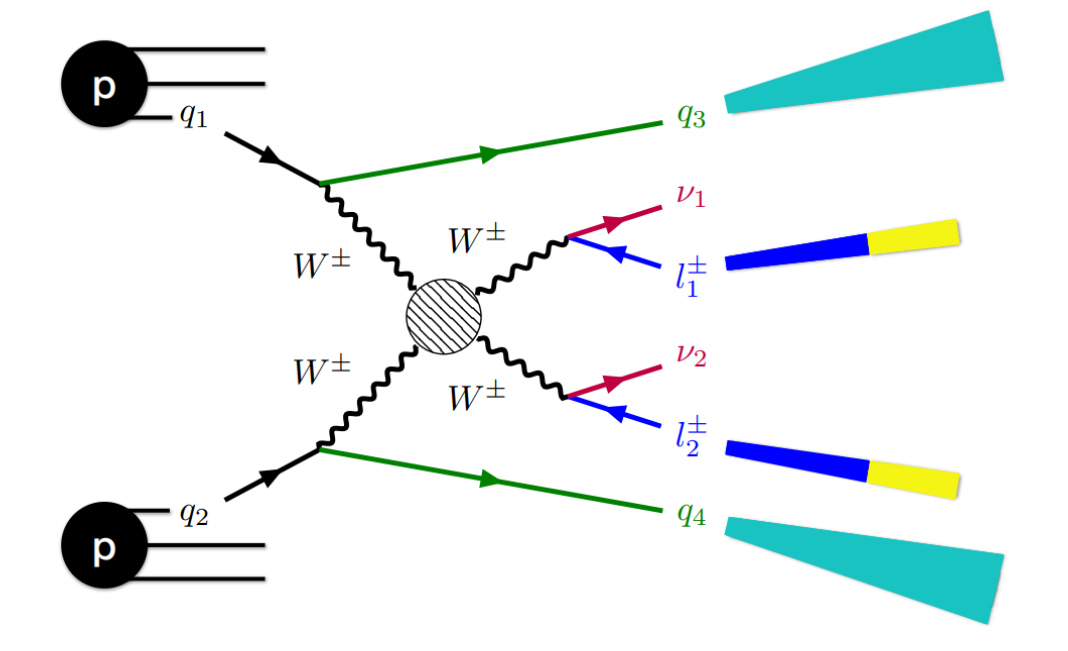
- Sig95% CL upper limit of 0.45 fb (expect 0.70 fb)
 - Most stringent limit of fully longitudinal polarized $W_L^{\pm}W_L^{\pm}jj-EW$
- Fiducial cross sections are measured, in agreement with the Stand Model
- Dominated by statistical uncertainty



Process	Predicet σB [fb]	Measured σB [fb]	Uncertainty
$W_L^{\pm}W_L^{\pm}jj$ $-EW$	0.29±0.07	0.01±0.21(tot)	$\pm 0.20(\text{stat})\pm 0.02(\text{mod.sys})\pm 0.06(\text{exp.sys})$
W _T ±W±jj − EW	2.56±0.64	3.39±0.35(tot)	$\pm 0.30(stat)\pm 0.08(mod.sys)\pm 0.16(exp.sys)$

Summary

- $W_L^{\pm}W_L^{\pm} \rightarrow W_L^{\pm}W_L^{\pm}$ is unique opportunity to probe EWSB
- State-of-the-art polarization prediction
 - Multi-jet merging in matrix element
 - NLO EW correction
- First evidence for longitudinal polairzation in vector boson scattering
- Most stringent limit of fully longitudinal polarized $W_L^{\pm}W_L^{\pm}jj-EW$
- Dominated by statistical uncertainty



Backup

2025/10/26

Object selection

Baseline and signal electron definition

Table 4.1: Baseline electron selection.

Identification: LooseLH Kinematic Acceptance: $p_T > 4.5 \text{ GeV}$ Geometrical Acceptance: $|\eta| < 2.47$ Longitudinal Impact parameter requirement: $|z_0 \times \sin \theta| < 0.5 \text{ mm}$ Transverse Impact parameter requirement: $\left| \frac{d_0}{\sigma_{d_0}} \right| < 5$ Isolation Requirement: none Table 4.2: Signal electron selection. Identification: TightLH Kinematic Acceptance: $p_T > 27 \text{ GeV}$ Geometrical Acceptance: $|\eta| < 2.47$, excluding $1.37 \le |\eta| \le 1.52$ Impact parameter requirements: as for preselection Isolation Requirement: Gradient Author==1Pass ECIDS

Baseline and signal muon definition

Table 4.3: Baseline muon selection.

Identification: Loose Kinematic Acceptance: $p_T > 3 \text{ GeV}$ Geometrical Acceptance: $|\eta| < 2.7$ Longitudinal Impact parameter requirement: $|z_0 \times \sin \theta| < 1.5 \text{ mm}$ Transverse Impact parameter requirement: $\left|\frac{d_0}{\sigma_{ch}}\right| < 15$ Isolation Requirement: none Table 4.4: Signal muon selection. Identification: Medium Kinematic Acceptance: $p_T > 27 \text{ GeV}$ Geometrical Acceptance: $|\eta| < 2.5$ Longitudinal Impact parameter requirement: $|z_0 \times \sin \theta| < 0.5 \text{ mm}$ Transverse Impact parameter requirement: $\frac{d_0}{\sigma_{do}} < 3$ Isolation Requirement: FixedCutPflowTight

- lepton in SR must pass the signal object selection
- Baseline objects are used to overlap removal and fake background yield estimation

2025/10/26 23

SR Cutflow

Cut name	WZEW	WZ QCD	Ch. Flip	Fakes	Other prompt	$V + \gamma$	ZZ	ssWW QCD	ss WW INT	$W_T W_T$	$W_T W_L$	W_LW_L
Channel Selection	4934.42 ± 2.94	215049.21 ± 138.80	366017848.00 ± 19131	-466834476.27 ± 1135	5383013.24 ± 533.49	226937481.05 ± 75581	175931.27 ± 119.98	1273.69 ± 1.14	158.14 ± 0.34	941.95 ± 0.59	472.62 ± 0.48	147.13 ± 0.13
GRL Selection	4934.42 ± 2.94	215049.21 ± 138.80	366017848.00 ± 19131	-466834476.27 ± 1135	5383013.24 ± 533.49	226937481.05 ± 75581	175931.27 ± 119.98	1273.69 ± 1.14	158.14 ± 0.34	941.95 ± 0.59	472.62 ± 0.48	147.13 ± 0.13
Jet Cleaning	4934.42 ± 2.94	215049.21 ± 138.80	365338053.00 ± 19113	-466834452.08 ± 1135	5383013.24 ± 533.49	226937481.05 ± 75581	175931.27 ± 119.98	1269.36 ± 1.14	157.64 ± 0.33	941.95 ± 0.59	472.62 ± 0.48	147.13 ± 0.13
Trigger Selection	4555.12 ± 2.83	177368.48 ± 127.23	220842708.00 ± 14860	-402085378.88 ± 1041	4636700.94 ± 497.13	195561497.48 ± 70574	156147.38 ± 118.29	1087.34 ± 1.05	134.54 ± 0.31	854.73 ± 0.56	427.80 ± 0.46	133.66 ± 0.12
Trigger Matching	4233.08 ± 2.70	164336.95 ± 117.27	213747311.00 ± 14620	-382938453.42 ± 1004	4305413.37 ± 474.26	186379871.06 ± 67950	146665.52 ± 104.31	1040.85 ± 1.02	128.56 ± 0.30	822.00 ± 0.55	410.96 ± 0.44	128.32 ± 0.12
Lepton (Anti)ID	3156.28 ± 2.34	125478.57 ± 104.69	144945418.00 ± 12039	-55971904.38 ± 38121	2557742.33 ± 370.24	140135492.96 ± 59872	110070.43 ± 93.52	742.49 ± 0.86	89.31 ± 0.26	623.12 ± 0.48	304.46 ± 0.38	94.40 ± 0.10
Apply Fake Factor	3156.28 ± 2.34	125478.57 ± 104.69	144945418.00 ± 12039	-8525418.48 ± 9092.2	2557742.33 ± 370.24	140135492.96 ± 59872	110070.43 ± 93.52	742.49 ± 0.86	89.31 ± 0.26	623.12 ± 0.48	304.46 ± 0.38	94.40 ± 0.10
lepton $p_T > 27$ GeV,												
$ \eta_{\mu} < 2.5$,	1958.09 ± 1.86	70370.05 ± 76.78	94687763.00 ± 9730.7	-5059554.65 ± 6359.6	1506136.44 ± 286.72	93057309.32 ± 51067.	60917.36 ± 47.20	413.96 ± 0.65	52.28 ± 0.20	378.17 ± 0.38	184.71 ± 0.30	59.10 ± 0.08
$ \eta_e < 1.37 \text{ in } ee$												
electron author	1958.09 ± 1.86	70370.05 ± 76.78	94687763.00 ± 9730.7	-5059554.65 ± 6359.6	1506136.44 ± 286.72	93057309.32 ± 51067.	60917.36 ± 47.20	413.96 ± 0.65	52.28 ± 0.20	378.17 ± 0.38	184.71 ± 0.30	59.10 ± 0.08
M11>20 GeV	1945.97 ± 1.86	69858.84 ± 76.66	94494590.00 ± 9720.8	-5058254.89 ± 6358.6	1490393.77 ± 285.25	93053805.74 ± 51067.	60800.43 ± 47.19	411.75 ± 0.65	51.90 ± 0.20	375.47 ± 0.37	183.46 ± 0.30	58.60 ± 0.08
Only two Leptons	578.15 ± 1.01	24900.84 ± 58.88	92823112.00 ± 9634.4	-4935263.93 ± 6304.7	1365158.30 ± 273.68	91471919.41 ± 50779.	45574.99 ± 44.36	393.81 ± 0.64	49.71 ± 0.20	363.02 ± 0.37	177.53 ± 0.29	56.88 ± 0.08
Truth- cut	552.44 ± 0.99	24871.92 ± 58.87	92823112.00 ± 9634.4	-4928825.06 ± 6301.9	1362565.00 ± 273.45	91447954.26 ± 50774.	33918.44 ± 37.35	392.97 ± 0.64	49.60 ± 0.20	362.23 ± 0.37	177.24 ± 0.29	56.81 ± 0.08
SS Leptons	92.54 ± 0.41	4757.80 ± 17.18	4299.44 ± 2.97	5671.80 ± 62.78	1028.96 ± 3.52	1237.33 ± 70.27	232.16 ± 1.44	392.94 ± 0.64	49.59 ± 0.20	362.21 ± 0.37	177.23 ± 0.29	56.80 ± 0.08
At least 2 jets with pT>65(35)GeV	66.17 ± 0.35	1123.88 ± 4.24	914.66 ± 2.08	2152.07 ± 30.23	865.16 ± 3.09	169.11 ± 7.19	33.21 ± 0.39	271.90 ± 0.53	43.42 ± 0.17	266.93 ± 0.32	126.53 ± 0.25	37.62 ± 0.07
Mij > 200 GeV	51.54 ± 0.31	612.45 ± 2.85	520.81 ± 1.62	1081.00 ± 21.61	431.66 ± 2.19	101.15 ± 5.21	18.21 ± 0.26	195.46 ± 0.45	39 53 + 0 16	234.93 ± 0.30	111.24 ± 0.23	34.38 ± 0.06
Z-Veto	50.11 ± 0.30	593.71 ± 2.80	284.62 ± 1.45	1032.96 ± 20.81	420.62 ± 2.16	74.04 ± 3.65	17.68 ± 0.26	192.38 ± 0.44	38.62 ± 0.16	229.95 ± 0.29	108.45 ± 0.23	33.31 ± 0.06
MET > 30 GeV	42.03 ± 0.28	494.89 ± 2.53	232.27 ± 1.33	846.53 ± 18.85	373.69 ± 2.02	54.32 ± 3.14	12.34 ± 0.21	169.75 ± 0.42	34.55 ± 0.15	204.89 ± 0.28	95.65 ± 0.22	28.28 ± 0.06
b-jet veto (85)	20.29 ± 0.20	397.79 ± 2.33	37.43 ± 0.54	259.82 ± 11.10	30.86 ± 0.59	41.73 ± 2.89	9.55 ± 0.19	140.12 ± 0.38	29.63 ± 0.14	180.70 ± 0.26	84.60 ± 0.20	25.36 ± 0.05
DYjj > 2	15.86 ± 0.17	213.73 ± 1.88	21.21 ± 0.42	144.55 ± 8.30	12.89 ± 0.42	24.63 ± 2.11	5.93 ± 0.16	48.38 ± 0.22	9.74 ± 0.09	162.24 ± 0.25	75.95 ± 0.19	23.50 ± 0.05
Mjj > 500 GeV	12.23 ± 0.15	82.75 ± 1.12	10.10 ± 0.31	56.31 ± 5.39	5.60 ± 0.28	10.55 ± 1.24	2.40 ± 0.09	24.05 ± 0.16	7.57 ± 0.08	141.84 ± 0.23	66.92 ± 0.18	20.56 ± 0.05
		02.70 2 1.112	10.10 2 0.01	20.21 2 2.27	5.00 2 0.20	10.00 2 1.21	2770 2 0107	2.1.00 2 0.110	2 0.00		001722 0110	20100 2 0100

2025/10/26